Chaos, Solitons and Fractals 201 (2025) 117236

Contents lists available at ScienceDirect

Chaos, Solitons and Fractals

journal homepage: www.elsevier.com/locate/chaos

The impact of time-weighted historical payoffs on evolution dynamics of strategies

Yanyan Han [a], Minlan Li [a,d], Xuemeng Song [d], Jia-Xu Han [d], Feng Zhang [c,*], Rui-Wu Wang [b,d,**]

[a] School of Mathematics and Statistics, Northwestern Polytechnical University, Xi'an, 710072, China
[b] College of Life Sciences, Zhejiang University, Zhejiang, 310058, China
[c] Yunnan Key Laboratory of Forest Ecosystem Stability and Global Change, Xishuangbanna Tropical Botanical Garden, Chinese Academy of Sciences, Mengla, 666303, Yunnan, China
[d] School of Ecology and Environment, Northwestern Polytechnical University, Xi'an, 710072, China

ARTICLE INFO

Keywords:
Fitness
Life stage
Resource flow
Historical payoffs
Replicator dynamics equation

ABSTRACT

Evolutionary game theory often oversimplifies fitness by equating it with immediate payoffs. This approach neglects biological realities, such as historical payoffs, resource storage, and metabolic transformation. This study addresses this gap by proposing a novel time-weighted fitness framework. This framework integrates these processes through a three-level structure: resource acquisition, cumulative fitness, and instantaneous fitness. This framework incorporates a maximum storable resource amount and three time-weighted modes (equal, decreasing, increasing) to simulate diverse life-history strategies. Analytical and numerical results reveal that time-weighted resource metabolism generates evolutionary dynamics inaccessible to the classical model. Decreasing time-weighting prioritizes early resource gains. This mode can induce persistent oscillations in strategy frequencies and strong path dependence, which aligns with capital breeding strategies. Increasing time-weighting, which amplifies recent resource gains, intensifies selection pressure over time, corresponding to terminal sprint strategies like pre-dormancy hyperphagia. When resources saturate, all dynamics revert to classical forms, signaling a strategic shift from capital accumulation to income competition. This work unifies historical contingency with instantaneous selection. It offers a mechanistic theory for interpreting diverse ecological patterns, from population cycles to life-history transitions.

1. Introduction

Evolutionary game theory provides a systematic framework for modeling the evolution of strategy frequencies in populations. In this framework, strategies are mapped to phenotypes, which are shaped by natural selection [1]. Mathematical tools such as replicator dynamics and spatial games are widely used in this field [2]. Fitness, a key concept linking ecological and evolutionary thought, is defined as the relative success of an organism in survival and reproduction. For decades, the standard modeling approach has been to equate fitness directly with the expected payoff (i.e., immediate resource gain) from interactions [3,4]. This assumption has proven

* Corresponding author.
** Correspondence to: R.-W. Wang, School of Ecology and Environment, Northwestern Polytechnical University, Xi'an, 710072, China.
E-mail addresses: fzhang@xtbg.ac.cn (F. Zhang), wangrw@zju.edu.cn (R.-W. Wang).

https://doi.org/10.1016/j.chaos.2025.117236
Received 1 July 2025; Received in revised form 10 September 2025; Accepted 13 September 2025
Available online 27 September 2025

fruitful. However, it is increasingly recognized as biologically oversimplistic, because it ignores the subsequent storage and metabolic transformation of these resources into fitness.

This conventional approach has two key limitations. Firstly, it disregards the fundamental biological processes of resource storage and metabolism. The approach treats payoffs as if they are instantly and entirely converted into reproductive output. In reality, organisms accumulate energy and nutrients over time and metabolize them at varying rates across life stages, subject to physiological constraints [5]. Secondly, it fails to account for the temporal heterogeneity in the value of resources. This value depends on the organism's life-history strategy, such as capital breeding or income breeding) [6]. Specifically, a unit of resource acquired early in a season may contribute far more to ultimate fitness than one acquired later, or vice versa.

Recent studies have focused on the temporal aspect, notably by introducing time delays [7–11] or memory functions [12–15] into payoff calculations. Tao and Wang pioneered the assumption that an individual's fitness at current time precisely depends on prior payoffs [9]. This work inspired a series of studies. For instance, Yuan and Meng analyzed fitness with time delay in the division of labor game [10], and Wettergren deconstructed the payoff matrixes to isolate benefit and cost delays [11]. However, such fixed delays often oversimplify the relationship between payoffs and fitness as linear. To model more complex relationships, studies have focused on recent payoffs. For example, Wang et al. [12] used power functions, Duan et al. [13] employed memory loss functions, and Li et al. [14] constructed exponential functions to weight payoffs within memory windows. Meanwhile, Ref. [15] demonstrated how time limitations can promote collaboration in structured populations. These approaches typically treat the weighted payoffs as direct, linear inputs for strategy updates. Moreover, they often fail to clearly formulate a concept of fitness or to establish a mechanistic link between weighted payoffs and resources. Notably, some studies have considered resource storage by treating weighted past payoffs as resource reserves that indirectly affect fitness [16–19]. In such models, immediate payoffs determine reserve growth, while time-accumulated payoffs form the basis of fitness. While these approaches acknowledge resources, they do not mechanistically model the metabolic transformation of resource reserve into fitness. Consequently, a unified framework that incorporates resource dynamics, temporal weighting, and physiological constraints into a mechanistic model of fitness is still lacking.

To bridge this gap, we introduce a novel three-level fitness framework that decouples the immediate payoff from its ultimate fitness contribution. Our model explicitly defines three levels. (i) Resource acquisition from payoffs. (ii) Cumulative fitness as the time-weighted metabolic integration of historical resource gains. (iii) Instantaneous fitness as the derivative of cumulative fitness. This derivative representing the real-time efficiency with which reserves are converted into selective advantages. This framework explicitly separates the acquisition of resources from its contribution to fitness. It thereby establishes a causal chain from payoffs (as resource gains) to stored reserves, then to metabolically integrated cumulative fitness potential, and finally to the instantaneous fitness that directly influences evolutionary selection via replicator dynamics. Moreover, this chain is aligned with biological realism by accounting for physiological constraints on resource storage and metabolic heterogeneity within a life stage. It embeds a maximum storable resource amount, creating two distinct metabolic pathways, and explores three time-weighted modes (equal, decreasing and increasing) to simulate different life-history strategies in a life stage.

Using this framework, we derive extended replicator dynamics and analyze them both theoretically and through numerical simulation. Our analysis reveals that time-weighted resource metabolism generates evolutionary dynamics inaccessible to classical models, such as persistent oscillations in strategy frequency. It also leads to strong path dependence, whereby initial conditions and historical resource advantages permanently influence evolutionary trajectories. Furthermore, when resource reserves reach saturation, time-weighted resource metabolism causes fundamental shifts in population strategies. This forces a transition between distinct life-history strategies, specifically from capital accumulation to income competition.

The paper is structured as follows. In Sec. 2, we develop the model, detailing the resource-storing mechanism and the derivation of time-weighted replicator dynamics. Section 3 presents a theoretical analysis of equilibria and stability, followed by numerical simulations of classic games. Section 4 gives conclusions and discussions.

2. Model

Building upon the limitations of classical models presented in the introduction, we now propose a novel theoretical framework that conceptualizes fitness across three interconnected levels. The first is resource acquisition via instantaneous payoffs. The second is cumulative fitness, defined as the metabolic integration of historical resources into survival and reproductive potential. The third is instantaneous fitness, which represents the real-time efficiency of converting reserves into selective advantages and serves as the immediate driver of frequency dynamics.

This framework explicitly includes physiological and environmental constraints by setting a maximum storable resource amount and creating two distinct metabolic pathways for resources. It also utilizes time-weighted functions to capture the temporal heterogeneity in resource value across life stages. The integration of these ecological and physiological realities allows us to derive extended replicator dynamics. These dynamics model a closed-loop feedback system that links payoffs, resource accumulation, metabolic transformation, fitness and strategy updates.

The following subsections develop this framework in detail. Section 2.1 models the resource-storing mechanism, Sec. 2.2 defines cumulative fitness and its derivative, and Sec. 2.3 derives the ensuing evolutionary dynamics.

2.1. Modeling resource acquisition and storage

Consistent with replicator dynamics (RD), we assume a well-mixed infinite population where individuals engage in randomized pairwise interactions and share the same strategy set $A = \{1, 2, \ldots, k\}$. At time t, let $n_i(t)$ $(i \in A)$ denote the number of individuals

choosing the strategy $i \in A$ and let $n(t) = \sum_{i \in A} n_i(t)$ be the total population size. The frequency of individuals choosing i-strategy is then $x_i(t) = n_i(t)/n(t)$. The profile $X(t) = [x_1(t), x_2(t), \ldots, x_k(t)]^T$ denotes the frequency distribution in the population, satisfying $X(t) \in \Omega_k$ for all time t, where $\Omega_k = \left\{ X = [x_1(t), x_2(t), \ldots, x_i(t)]^T \middle| \sum_{i=1}^{k} x_i(t) = 1 \text{ and } x_i(t) \geq 0 \right\}$ is a simplex that depends on the number of strategies k. At each time t within a life stage, let $\pi_{i,j}$ denote the payoff to an individual adopting i-strategy when interacting with one adopting j-strategy. The expected payoff of i-strategy at time t is thus $f_i(X(t)) = \sum_{j \in A} \pi_{i,j} x_j(t)$.

In ecology, the objective of games among individuals typically centers on resource acquisition. This is because resources serve as the fundamental currency for enhancing fitness, through their roles in supporting survival and reproduction. Accordingly, we define the expected payoff for i-strategy as a resource gain, denoted $\Delta E_i(t) = f_i(X(t))$. We assume that individuals update their strategies not based on this immediate gain, but on their resource reserves $E_i(t)$, which represent the time-accumulated resources. The value of $E_i(t)$ quantifies the average reserve across all individuals adopting i-strategy at time t, and its dynamics are given by

$$\frac{dE_i(t)}{dt} = \begin{cases} \Delta E_i(t), & \text{when } E_i(t) < K, \\ 0, & \text{when } E_i(t) \geq K, \end{cases}$$

where $\Delta E_i(t)$ is the resource gain of i-strategy at time t. Due to physiological and environmental constraints, individuals cannot accumulate resources infinitely within a life stage. Therefore, we impose a maximum storable amount, K. When $E_i(t) < K$, individuals store new resource gains to increase reserves. Otherwise, they cease storage.

This maximum amount K is defined as the maximum reserve an individual can accumulate within the life stage duration. Specifically, $K = \lambda \cdot T \cdot R_{max}$, where T is the life stage duration, R_{max} is the maximum payoff per game, and λ ($0 < \lambda < 1$) is the storage efficiency coefficient accounting for inevitable metabolic losses during assimilation, maintenance costs, and other energetic overheads [20]. This formulation confirms that K is not merely a physical constraint but also a reflection of an individual's metabolic efficiency.

2.2. Defining cumulative fitness via metabolism transformation

Traditional evolutionary game models assume that resources are immediately converted into fitness. However, in reality, individuals first store resources with a life stage until reaching the maximum K. Furthermore, all resource gains, whether stored or not, require metabolic transformation to generate survival and reproductive potential. Based on Ref. [5], we assert that fitness emerges from the metabolic transformation of acquired resources into survival and reproductive output. We therefore define the cumulative fitness $F_i(t)$ as the total survival and reproductive potential generated up to time t. This potential is derived from the metabolic transformation of all acquired resources, regardless of their storage path. Here, $F_i(t)$ represents the average cumulative fitness potential across all individuals adopting i-strategy. Unlike the lifetime fitness, which considers an individual's survival and reproductive success across its entire life cycle, the proposed cumulative fitness $F_i(t)$ is confined to a single life stage. It provides a snapshot of resource metabolism and fitness potential at that stage. However, both embody fitness as a long-term outcome of resource metabolism.

As described in Sec. 2.1, there is a maximum amount to resource reserves, which leads to two resource flow paths. When the reserve is below the maximum K, new resource gains are stored and gradually metabolized into cumulative fitness contributions. When the reserve reaches the maximum K, excess resource gains bypass storage and are immediately and fully metabolized, contributing directly to the cumulative fitness at the moment they are acquired. This duality means that $F_i(t)$ naturally couples historical contributions from resource reserves and immediate contributions from excess resources.

The contribution of resource reserves to the cumulative fitness $F_i(t)$ depends on their cumulative metabolic effect within a given stage. This effect is shaped by temporal heterogeneity in resource acquisition. Specifically, individuals metabolize reserves at different times to meet their immediate needs. Consequently, resource gains acquired at different times make unequal contributions to $F_i(t)$. This reflects the temporal heterogeneity in resource value, where the worth of a stored resource unit depends on when it is mobilized and utilized [25]. Our model focuses on the evolutionary dynamics within a specific life stage, such as a breeding season, hibernation period or dry season. During this stage, organisms typically exhibit a consistent metabolic strategy, which serves as a core premise for defining the time-weighted function $\delta(t, \tau)$. It ensures the time-weighted rule of resource value remains stable throughout the stage, rather than being disrupted by cross-stage metabolic changes. Thus, the time-weighted function$\delta(t, \tau)$ is designed to capture this temporal heterogeneity in resource value within a single life stage. It quantifies how the timing τ of a resource gain influences the fitness potential at a later time t. For the resource reserves, the cumulative fitness is calculated as $F_i(t) = F_i(0) + \int_0^t \delta(t, \tau) \Delta E_i(\tau) d\tau$, where the initial cumulative fitness $F_i(0) = 0$ in this stage. Here, $\delta(t, \tau)$ unifies the stage-specific metabolic efficiency and the temporal heterogeneity of resource value, directly linking the timing of resource gains to its actual contribution to fitness potential. We propose three modes for $\delta(t, \tau)$:

- The fixed weighting mode, where $\delta(t, \tau) = 1$, assumes an equal contribution of resource gains. It applies to environments or life stages with constant and persistent resource needs, where there is no physiological or ecological reason to value resources from one time over another. This represents a baseline null model and may describe species with minimal seasonal variation in their metabolic priorities. It corresponds to the equally time-weighted cumulative fitness $F_i^1(t) = \int_0^t \Delta E_i(\tau) d\tau$.
- The decreasing time-weighting mode $\delta(t, \tau) = t - \tau$ is motivated by the life-history strategies of species such as Svalbard reindeer. In their annual cycle, body condition and fat reserves accumulated during the short summer are critically important for surviving the harsh winter and succeeding in reproduction the following spring [21]. This creates a strong biological precedent for prioritizing

early resource gains. A unit acquired early in the season contributes far more to cumulative fitness than one acquired later, supporting a linearly decreasing weighting scheme. This theoretical premise is supported by empirical evidence from long-term ecological studies. For instance, research on ungulates has quantitatively demonstrated that early-life resource acquisition (e.g., body condition in first year) significantly impacts lifetime reproductive success [22]. This mode corresponds to the decreasingly time-weighted cumulative fitness $F_i^2(t) = \int_0^t (t-\tau)\Delta E_i(\tau)d\tau$.

- The increasing time-weighting mode $\delta(t,\tau) = \tau$ is motivated by the physiological strategies of hibernating mammals [23]. For species such as bears, a phase of hyperphagia precedes dormancy. During this critical phase, metabolic pathways are upregulated to maximize the efficiency of converting recent energy intake into fat stores [24]. Therefore, resources acquired in this narrow window immediately before hibernation are metabolically prioritized and are essential for successfully initiating and sustaining torpor, supporting vital functions, and facilitating gestation throughout the winter. This creates a clear biological rationale for a linearly increasing weighting scheme. A unit of resource gained late in this stage contributes more to the animal's overwinter survival and reproductive potential than an identical unit gained earlier. This mode corresponds to the increasingly time-weighted cumulative fitness $F_i^3(t) = \int_0^t \tau\Delta E_i(\tau)d\tau$.

These specific linear forms of $\delta(t,\tau)$ are chosen as a foundational step to establish the core principle of time weighting. Their mathematical simplicity makes them analytically tractable and offers the clearest possible illustration of how prioritizing early versus recent gains can fundamentally alter evolutionary dynamics. While nonlinear functions (e.g., exponential decay or sigmoidal shapes) may describe specific systems more accurately, these canonical linear cases are sufficient to capture the essential qualitative differences and generate novel, testable predictions.

When the reserve $E_i(t)$ reaches the maximum K at time t_1 ($t_1 < T$), any excess resource gains bypass storage and are immediately and fully metabolized. These excess resources contribute directly to the cumulative fitness $F_i(t)$ at the moment they are acquired. Thus, the cumulative fitness naturally incorporates contributions from two distinct resource flow paths, storage-dependent metabolism and immediate metabolism of excess. The implications of this duality vary by time-weighting mode. For the equally time-weighted cumulative fitness $F_i^1(t) = \underbrace{\int_0^{t_1} \Delta E_i(\tau)d\tau}_{\text{reserve contribution}} + \underbrace{\int_{t_1}^{t} \Delta E_i(\tau)d\tau}_{\text{excess gain contribution}}$, all resources contribute equally, reflecting a balanced reliance on past and present gains. For the decreasingly time-weighted cumulative fitness $F_i^2(t) = \underbrace{\int_0^{t_1} (t-\tau)\Delta E_i(\tau)d\tau}_{\text{reserve contribution}} + \underbrace{\int_{t_1}^{t} \Delta E_i(\tau)d\tau}_{\text{excess gain contribution}}$, early stored resources remain critically important for long-term needs. And, for the increasingly time-weighted cumulative fitness $F_i^3(t) = \underbrace{\int_0^{t_1} \tau\Delta E_i(\tau)d\tau}_{\text{reserve contribution}} + \underbrace{\int_{t_1}^{t} \Delta E_i(\tau)d\tau}_{\text{excess gain contribution}}$, recently stored resources are most valuable for meeting impending demands in this life stage.

Having defined cumulative fitness $F_i(t)$ as the integral of time-weighted resource gains, we must determine which measure drives selection in RD. While $F_i(t)$ quantifies the total potential derived from past resource, the biologically correct basis for evolutionary dynamics is its time derivative. This is defined as the instantaneous fitness $(F_i(t))'$. This distinction rests on two principles, including physiological constraint and the mechanism of natural selection.

From a physiological perspective, $F_i(t)$ measures the total resource potential but fails to capture the real-time rates of resource mobilization, which are constrained by metabolism. For example, Svalbard reindeer (capital breeders) cannot instantly convert their substantial summer fat reserves into advantages for survival in winter. The conversion rate is limited by enzymatic activity [25]. Similarly, once the maximum amount K is reached, any excess resources are directly metabolized. This process is not reflected in the static total $F_i(t)$, but in the dynamic derivative $(F_i(t))'$. This derivative quantifies the real-time metabolic rate, such as the efficiency of fat catabolism at a given moment.

Natural selection acts on immediate differences in survival and reproduction. From this perspective, the relevant driver is $(F_i(t))'$. The overwinter survival of a hibernator depends not on its total pre-hibernation reserves $F_i(t)$, but on the rate at which those reserves are converted into energy $(F_i(t))'$ during dormancy. Consequently, even two strategies with identical cumulative fitness $F_i(t)$ will be distinguished by selection if their instantaneous metabolic efficiencies $(F_i(t))'$ differ. Using $F_i(t)$ directly would obscure this vital selective signal.

In summary, $F_i(t)$ represents the comprehensive potential of historical resources, while $(F_i(t))'$ represents its real-time expression as fitness. This distinction is consistent with the physiology of resource metabolism and the action of natural selection. Therefore, the extended RDs must be derived using $(F_i(t))'$, as detailed in the following section.

2.3. Deriving the strategy dynamics from cumulative fitness

In classical evolutionary game theory, changes in strategy frequency are driven by the difference between immediate payoffs. However, in our framework, the immediate expected payoff $f_i(t)$ is interpreted as a resource gain, which must be metabolically

transformed into fitness potential. Therefore, a more biologically grounded approach should base the evolutionary dynamics on the cumulative outcome $F_i(t)$ of this transformation process. $F_i(t)$ couples the entire history of resource acquisition and metabolism up to time t.

To characterize how the cumulative fitness influences the evolution of strategies, a mapping from this accumulated potential to changes in strategy frequency is required. This mapping is achieved using the Logit choice rule [26,27], a standard function for modeling bounded rational decision-making. According to this rule, the frequency $x_i(t)$ of i-strategy is given by

$$x_i(t) = \frac{\exp(\beta F_i(t))}{\sum_{j\in A}\exp(\beta F_i(t))}, \tag{1}$$

where $\beta(>0)$ is the intensity of selection modulated. This ensures $x_i(t) \in [0,1]$ and $\sum_{i=1}^{k} x_i(t) = 1$. The rule posits that strategies with higher cumulative fitness are adopted with higher probability in an exponential manner.

To derive the continuous-time dynamics, we differentiate Eq. (1) with respect to time t. Applying the quotient rule and simplifying, we obtain the following RD

$$\begin{aligned}
x_i^{'}(t) &= \left(\frac{\exp(\beta F_i(t))}{\sum_{j\in A}\exp(\beta F_i(t))}\right)^{'} \\
&= \frac{\exp(\beta F_i(t))\left[\beta(F_i(t))^{'}\left(\sum_{j\in A}\exp(\beta F_j(t))\right) - \left(\sum_{j\in A}\exp(\beta F_j(t))\beta(F_j(t))^{'}\right)\right]}{\left(\sum_{j\in A}\exp(\beta F_j(t))\right)^{2}} \\
&= x_i(t)(\beta F_i(t))^{'} - x_i(t)\sum_{j\in A}x_j(t)\beta(F_j(t))^{'} \\
&= \beta x_i(t)\left((F_i(t))^{'} - \sum_{j\in A}x_j(t)(F_j(t))^{'}\right),
\end{aligned}$$

where $(F_i(t))^{'}$ is the instantaneous fitness, representing the real-time efficiency of converting resource reserves into survival and reproductive advantages per unit time. The term $\sum_{j\in A}x_j(t)(F_j(t))^{'}$ is the population average instantaneous fitness. The parameter β (>0) scales the intensity of selection. Since it is a positive constant that modulates the rate of evolution without altering the equilibrium or the qualitative dynamics of the system, we can simplify the equation by rescaling time. Defining a new time scale $\tau = \beta \cdot t$, the equation reduces to the canonical form of RD. For notational simplicity and to facilitate comparison with classical results, we use this β-free form in the subsequent analysis

$$x_i^{'}(t) = x_i(t)\left((F_i(t))^{'} - \sum_{j\in A}x_j(t)(F_j(t))^{'}\right). \tag{2}$$

This derivation leads to a critically important result. Although the strategy frequency $x_i(t)$ depends on the comprehensive history of resource metabolism $F_i(t)$, the resulting change in population strategy frequencies is driven instantaneously by the derivative of this history $(F_i(t))^{'}$, i.e., the current efficiency of converting reserves into advantages. This elegantly reconciles two seemingly opposed principles. Historical contingency is embedded in the cumulative fitness $F_i(t)$ and instantaneous natural selection is driven by the derivative $(F_i(t))^{'}$. The entire history of payoffs exerts its influence on present-day evolution by shaping the current physiological state upon which selection acts.

For the equally time-weighted cumulative fitness $F_i^1(t) = \int_0^{t_1} f_i(X(\tau))d\tau + \int_{t_1}^{t} f_i(X(\tau))d\tau$, the instantaneous fitness is equal to the immediate payoff $\left(F_i^1(t)\right)^{'} = f_i(t)$, regardless of the resource reserve. Substituting this into Eq. (2) yields

$$\begin{aligned}
x_i^{'}(t) &= x_i(t)\left(\left(F_i{}^1(t)\right)^{'} - \sum_{j\in A}x_j(t)\left(F_j{}^1(t)\right)^{'}\right) \\
&= x_i(t)\left(f_i(t) - \sum_{j\in A}x_j(t)f_j(t)\right).
\end{aligned} \tag{3}$$

This RD recovers the classical dynamics proposed by Taylor and Jonker [3]. The equivalence arises because the equal weighting mode assumes constant metabolic efficiency and persistent resource needs over time. In this context, a unit of resource gained in the past has the same value as a unit gained now. Therefore, the historical legacy of resource accumulation $E_i(t)$ provides no relative advantage, and selection depends solely on the immediate rate of resource acquisition $f_i(t)$, precisely as in classical theory. This mode effectively describes systems in stable environment with minimal temporal discounting of resource value. For the subsequent analysis,

we focus on the two-strategy case $k = 2$. With the strategy set $A = \{1, 2\}$, we let $x(t)$ denote the frequency of 1-strategy and $1 - x(t)$ the frequency of 2-strategy. The RD then simplifies to

$$x'(t) = x(t)(1 - x(t))(f_1(t) - f_2(t)). \tag{4}$$

For the decreasingly time-weighted cumulative fitness $F_i^2(t) = \int_0^{t_1} (t-\tau) f_i(X(\tau))d\tau + \int_{t_1}^{t} f_i(X(\tau))d\tau$, two distinct cases arise based on resource saturation. When the resource reserve is below the maximum K at time t, the instantaneous fitness is $\left(F_i^2(t)\right)' = \int_0^t f_i(\tau)d\tau$. Substituting this into Eq. (2) yields the first-order dynamics

$$\begin{aligned} x_i'(t) &= x_i(t)\left(\left(F_i^2(t)\right)' - \sum_{j\in A} x_j(t)\left(F_j^2(t)\right)'\right) \\ &= x_i(t)\left(\int_0^t f_i(\tau)d\tau - \sum_{j\in A} x_j(t)\int_0^t f_j(\tau)d\tau\right). \end{aligned} \tag{5}$$

This system is non-autonomous and analytically challenging. To enable standard analysis, we differentiate it to obtain an autonomous second-order RD, as following

$$\begin{aligned} x_i''(t) &= \left(x_i(t)\left(\left(F_i^2(t)\right)' - \sum_{j\in A} x_j(t)\left(F_j^2(t)\right)'\right)\right)' \\ &= x_i'\left(\left(F_i^2(t)\right)' - \sum_{j\in A} x_j\left(F_j^2(t)\right)'\right) - x_i\left(\sum_{j\in A} x_j'\left(F_j^2(t)\right)'\right) + x_i\left(\left(F_i^2(t)\right)'' - \sum_{j\in A} x_j\left(F_i^2(t)\right)''\right). \end{aligned}$$

Substituting $\frac{x_i'(t)}{x_i(t)} = \left(\left(F_i^2(t)\right)' - \sum_{j\in A} x_j\left(F_j^2(t)\right)'\right)$ and $\left(F_i^2(t)\right)'' = f_i(t)$ into this, we get

$$x_i''(t) = x_i'(t)\frac{x_i'(t)}{x_i(t)} - x_i(t)\left(\sum_{j\in A} x_j'(t)\left(F_j^2(t)\right)'\right) + x_i(t)\left(f_i(t) - \sum_{j\in A} x_j(t) f_j(t)\right),$$

then combining like terms by adding/subtracting the same term $x_i \sum_{k\in A} x_k'\left(\sum_{j\in A} x_j\left(F_j^2(t)\right)'\right)$. It gives

$$x_i''(t) = x_i\left(f_i(t) - \sum_{j\in A} x_j f_j(t)\right) - x_i \sum_{k\in A} x_k'\left(\sum_{j\in A} x_j\left(F_j^2(t)\right)'\right) + x_i\left(\frac{\left(x_i'\right)^2}{(x_i)^2} - \sum_{k\in A} x_k'\left(\left(F_k^2(t)\right)' - \sum_{j\in A} x_j\left(F_j^2(t)\right)'\right)\right), \quad \text{where}$$

$\left(\sum_{j\in A} x_j\left(F_j^2(t)\right)'\right)$ is irrelevant to k and $\sum_{k\in A} x_k'(t) = 0$ (because the sum of strategy frequencies is always 1, its derivative must be 0), so the second-order RD is

$$x_i''(t) = x_i(t)\left(f_i(t) - \sum_{j\in A} x_j(t) f_j(t)\right) + x_i(t)\left(\frac{\left(x_i'(t)\right)^2}{\left(x_i(t)\right)^2} - \sum_{k\in A}\frac{\left(x_k'(t)\right)^2}{x_k(t)}\right). \tag{6}$$

This RD reveals a profound shift in selective pressure. The instantaneous fitness is now determined by the average historical resource reserve $\int_0^t f_i(\tau)d\tau$, not the current intake $f_i(\tau)$. This embodies the strategy of a capital breeder or a seasonal survivor, where success is contingent on building a large reserve early on. The nonlinear term in Eq. (6) captures the long-lasting, inertial effect of early resource advantages, i.e., a head start that continues to pay dividends into the future. Ecologically, this aligns with organisms like Svalbard reindeer, where body condition established in summer is the primary determinant of winter survival and subsequent reproductive success.

When the resource reserve reaches the maximum K at time t_1, the instantaneous fitness becomes $\left(F_i^2(t)\right)' = \int_0^{t_1} f_i(\tau)d\tau + f_i(t)$. Substituting this into Eq. (2) yields

$$\begin{aligned} x_i'(t) &= x_i(t)\left(\left(F_i^2(t)\right)' - \sum_{j\in A} x_j(t)\left(F_j^2(t)\right)'\right) \\ &= x_i(t)\left(\int_0^{t_1} f_i(\tau)d\tau + f_i(t) - \sum_{j\in A} x_j(t)\left(\int_0^{t_1} f_j(\tau)d\tau + f_j(t)\right)\right). \end{aligned} \tag{7}$$

Although Eq. (7) mathematically similar to the classical form, its biological interpretation signifies a complete strategic reversal. Individuals can no longer gain advantage from their historical capital, as early resource advantages are frozen in the constant integral term $\int_0^{t_1} f_i(\tau)d\tau$. Selection pressure abruptly shifts to favor phenotypes that maximize immediate resource acquisition and consumption efficiency $f_i(t)$. A strategy dominant in the accumulation phase may be supplanted if it is not superior in this new saturated environment of pure income breeding. This illustrates an ecological scenario where early success does not guarantee long-term dominance if conditions change. For the two-strategy case $A = \{1, 2\}$, with $x(t) = x_1(t)$ and $1 - x(t) = x_2(t)$, the dynamics in the unsaturated and saturated cases simplify to

$$\begin{cases} x''(t) = x(t)(1-x(t))(f_1(t)-f_2(t)) + \dfrac{1-2x(t)}{x(t)(1-x(t))}x'(t)^2, \text{when } E_1(t) < K, \\ x'(t) = x(t)(1-x(t))\left(\displaystyle\int_0^{t_1}(f_1(\tau)-f_2(\tau))d\tau + f_1(t)-f_2(t)\right), \text{when } E_1(t) \geq K. \end{cases} \tag{8}$$

For the increasingly time-weighted cumulative fitness $F_i^3(t) = \int_0^{t_1} \tau f_i(X(\tau))d\tau + \int_{t_1}^{t} f_i(X(\tau))d\tau$, the analysis again separates into two cases based on resource saturation. When the resource reserve is below the maximum K, the instantaneous fitness is $\left(F_i^3(t)\right)' = tf_i(X(t))$. Substituting this into Eq. (2) yields

$$\begin{aligned} x_i'(t) &= x_i(t)\left(\left(F_i^3(t)\right)' - \sum_{j\in A} x_j(t)\left(F_j^3(t)\right)'\right) \\ &= x_i(t)\left(tf_i(t) - \sum_{j\in A} x_j(t)tf_j(t)\right). \end{aligned} \tag{9}$$

Here, the instantaneous fitness amplifies the value of reserves by a time-dependent factor t. This creates a strong selective pressure that rewards recent success, effectively modeling the physiology of pre-dormancy hyperphagia in hibernators. As a critical life-stage event (e.g., hibernation) approaches, the metabolic system becomes highly efficient at processing incoming resources. Consequently, a unit of resources gained immediately before the event has a far greater impact on fitness than a unit gained long before. These dynamics prioritizes strategies that excel at late-stage, high-efficiency foraging.

When the maximum K is reached at time t_1, the instantaneous fitness simplifies to the immediate payoff $\left(F_i^3(t)\right)' = f_i(X(t))$. Substituting into Eq. (2) yields the classical RD

$$\begin{aligned} x_i'(t) &= x_i(t)\left(\left(F_i^3(t)\right)' - \sum_{j\in A} x_j(t)\left(F_j^3(t)\right)'\right) \\ &= x_i(t)\left(f_i(t) - \sum_{j\in A} x_j(t)f_j(t)\right). \end{aligned} \tag{10}$$

The reversion of the classical form in Eq. (10) signifies a critical phenotypic shift from capital accumulation to pure income consumption. For species employing this strategy (e.g., hibernators), reaching saturation often triggers a profound physiological transition, such as entering dormancy, where active foraging ceases. The crucial evolutionary insight is that the saturating point t_1 marks the end of the investment phase. The total capital $F_i^3(t) = \int_0^{t_1} \tau f_i(X(\tau))d\tau$ available for the ensuing physiological challenge (e.g., hibernation) is determined by the trajectory up to that point t_1. For the two-strategy case $A = \{1,2\}$, with $x(t) = x_1(t)$ and $1 - x(t) = x_2(t)$, the dynamics simplify to

$$\begin{cases} x'(t) = x(t)(1-x(t))(tf_1(t) - tf_2(t)), \text{when } E_1(t) < K, \\ x'(t) = x(t)(1-x(t))(f_1(t) - f_2(t)), \text{when } E_1(t) \geq K. \end{cases} \tag{11}$$

In summary, the extended RDs (4), (8), and (11) describes three distinct metabolic modes for converting resources into fitness, prioritizing equal, early, or recent resource gains. While these RD preserve the core principle that natural selection acts on instantaneous differences in survival and reproduction $(F_i(t))'$, they extend the classical theory by introducing how historical resource gains $F_i(t)$ shape the physiological state upon which selection acts.

This creates a closed feedback loop. The payoffs determine resource gains, which are metabolically integrated into cumulative fitness. The derivative of this cumulative fitness then drives changes in strategy frequency, which in turn determines future payoffs. Thus, this framework quantifies how long-term adaptive strategies emerge from the dynamics interplay between instantaneous selection pressures and the legacy of past resource acquisition.

3. Results

3.1. Equilibrium and stability analysis of two-strategy dynamics

In this section, we analyze the equilibrium and their stability for the two-strategy replicator dynamics (RD) derived in Sec. 2.3. Here, we denote the payoff matrix $M = \begin{pmatrix} a & b \\ c & d \end{pmatrix}$, where a player using 1-strategy gets payoff a against another player using 1-strategy and gets payoff b against another player using 2-strategy; a player using 2-strategy gets payoff c against another player using 1-strategy, and gets payoff d against another player using 2-strategy. At time t, the frequency choosing 1-strategy is $x(t)$ and the frequency choosing 2-strategy is $1 - x(t)$. Hence, the expected payoff choosing 1-strategy is $f_1(t) = (a-b)x(t) + b$ and the expected payoff choosing 2-strategy is $f_2(t) = (c-d)x(t) + d$. Then, we consider the dynamical behaviors of each RD, under the three assumptions on $\delta(t,\tau)$ mentioned in Sec. 2.

For the equally time-weighted RD (4), it has three equilibria $E_1^*(0,1)$, $E_2^*(1,0)$, $E_3^*\left(\frac{d-b}{a-b-c+d}, \frac{a-c}{a-b-c+d}\right)$ ($\in [0,1]$, $a-b-c+d \neq 0$),

according to Ref. [28]. E_1^* is a stable node if $b < d$ *or* $b = d\&a < c$, otherwise it is an unstable node. E_2^* is a stable node if $c < a$ *or* $a = c\&b > d$, otherwise it is an unstable node. And, E_3^* is a stable node if $a < c\&d < b$ and it is a saddle if $a > c\&d > b$, otherwise E_3^* does not exist in the RD. Moreover, around the stable equilibria, the linearization system is given

$x^{'}(t)|_{(x^*1-x^*)} = [(1-2x^*)((a-b-c+d)x^* + (b-d)) + (a-b-c+d)x^*(1-x^*)](x(t)-x^*) = g_1^{'}(x^*)(x(t)-x^*)$.Its solution is $x(t) = x^* + (x(0)-x^*)\exp\left(g_1^{'}(x^*)t\right)$ and then the convergence rate is exponentially related to time and is determined by the eigenvalue $g_1^{'}(x^*)$.

According to the RD (4) settings in Sec. 2.2, when the resource reserve $E_1(t)$ reaches its maximum amount K, the fitness $\left(F^1(t)\right)^{'} = f(t)$ is identical to the classical RD. Thus, its equilibrium states and stability characteristics are identical to the analysis results when $E_1(t) < K$. This confirms that in ecological contexts where the value of a resource unit is constant over time in stable, non-seasonal environments, the historical time-weighting of resources provides no additional selective advantage. Evolution proceeds as if payoffs are immediately converted into fitness, and the long-term outcome is determined solely by the matrix M. The dynamics serve as a valuable null model against which the more complex time-weighted dynamics can be compared.

For the decreasingly time-weighted RD (8), we first consider the case where $E_1(t) < K$. This is usually done by converted it into a one-order system by letting $y = x^{'}$ and is written as

$$\begin{cases} x^{'}(t) = y(t), \\ y^{'}(t) = x(t)(1-x(t))[(a-b-c+d)x(t) + (b-d)] + \dfrac{1-2x(t)}{x(t)(1-x(t))}y(t)^2. \end{cases} \tag{12}$$

At the equilibria, $y^* = 0$ and the nonlinear term $\frac{1-2x^*}{x^*(1-x^*)}y^{*2} = 0$ holds, the equilibria only need to satisfy $x(1-x)[(a-b-c+d)x + (b-d)] = 0$, that is, $x_1^* = 0, x_2^* = 1$ and $x_3^* = \frac{d-b}{a-b-c+d}(\in (0,1), a-b-c+d \neq 0)$. So, in the RD (8), the equilibria are still E_1^*, E_2^*, E_3^*. Let $g_1(x) = x(1-x)[(a-b-c+d)x + (b-d)]$ and $g_2(x) = \frac{1-2x}{x(1-x)}$, $y^{'} = g_1(x) + g_2(x)y^2$ and the Jacobi matrix $J = \begin{bmatrix} 0 & 1 \\ g_1{}^{'}(x^*) & 0 \end{bmatrix}$, so it gives eigenvalues $\eta_{1,2} = \pm\sqrt{g_1{}^{'}(x^*)}$. Note that for an equilibrium acting as a center in the linearized system, the nonlinear terms $g_2(x)y^2$ must be considered.

- For $x_1^* = 0$, it gives $\eta_{1,2} = \pm\sqrt{b-d}$. When $b-d > 0$, $\eta_{1,2}$ are two real roots with opposite signs, and $(0,0)$ is a saddle in the system (12). When $b-d < 0$, $\eta_{1,2}$ are purely imaginary, and $(0,0)$ is a center in the linearized system. This requires further analysis. In the neighborhood of $(0,0)$, it gives $g_1(x) \approx (b-d)x, g_2(x) \approx 1/x$ and then makes the system (12) approximate as $\begin{cases} x^{'} = y \\ y^{'} \approx (b-d)x + \dfrac{y^2}{x} \end{cases}$. Setting $b-d = -\beta(\beta > 0)$ and $v = y/x(y = vx)$, the approximate system becomes $y^{'} \approx -\beta x + \frac{y^2}{x} = -\beta x + v^2 x$. Combining $y^{'} = v^{'}x + vx^{'} = v^{'}x + vy = v^{'}x + v^2 x$, we know that $v^{'} = -\beta$, so the exact solution is $\begin{cases} v(t) = v(0) - \beta t \\ x(t) = x(0)\exp\left(\int_0^t v(s)ds\right) = x(0)\exp\left(v(0)t - \dfrac{\beta}{2}t^2\right) \end{cases}$. Therefore, when $t \to \infty$, $y(t) = v(t)x(t) = (v(0)-\beta t)x(0)\exp\left(v(0)t - \frac{\beta}{2}t^2\right) \to 0$, $x(t) \propto \exp\left(-\beta/2t^2\right) \to 0$, causing $x(t)$ and $y(t)$ to converge to 0 with super-exponential decay. Moreover, when $(x,y) \to (0,0)$, $v(t) = v(0) - \beta t = \frac{y(t)}{x(t)} \to -\infty$ along trajectories, so the vertical tangent line $\frac{dy}{dx} = -\beta\frac{x}{y} + \frac{y}{x} \approx \frac{y}{x} \to -\infty$ forces trajectories to enter $(0,0)$ along the negative y-axis, forming an asymptotically stable node.
- For $x_2^* = 1$, it gives eigenvalues $\eta_{1,2} = \pm\sqrt{c-a}$. When $c-a > 0$, $(1,0)$ is a saddle in the system (12). When $c-a < 0$, $(1,0)$ is a center in the linearized system. Naturally, by using the same analysis as above, it can be proved that all trajectories enter $(1,0)$ along the positive y-axis to form an asymptotic stable node.
- For $x_3^* = \frac{d-b}{a-b-c+d}$, it gives eigenvalues $\eta_{1,2} = \pm\sqrt{\frac{(d-b)(a-c)}{(a-b-c+d)}}$. When $a-b-c+d > 0$ $(a > c\&d > b)$, $\left(\frac{d-b}{a-b-c+d}, 0\right)$ is a saddle in the system (12). When $a-b-c+d < 0$ $(a < c\&d < b)$, $\left(\frac{d-b}{a-b-c+d}, 0\right)$ is a center in the linearized system. Here, we apply a time-reversal transformation to the system (12). Let $\iota = -t$, $\frac{dx}{dt} = -\frac{dx}{d\iota}$ and $\frac{dy}{dt} = -\frac{dy}{d\iota}$, which transforms the system (12) into $\begin{cases} \dfrac{dx}{d\iota} = -y, \\ \dfrac{dy}{d\iota} = -g_1(x) - g_2(x)y^2. \end{cases}$ Moreover, there exists an involution mapping $R(x,y) = (X,-Y)$ such that the transformed system

$\begin{cases} \frac{dX}{dt} = -y = -(-Y) = Y, \\ \frac{d(-Y)}{dt} = -g_1(x) - g_2(x)y^2 = -g_1(X) - g_2(X)(-Y)^2, \end{cases}$ so $\begin{cases} \frac{dX}{dt} = Y, \\ \frac{dY}{dt} = g_1(X) + g_2(X)Y^2. \end{cases}$ becomes identical to the system (12). By the central theorem of reversible systems [29], $\left(\frac{d-b}{a-b-c+d}, 0\right)$ remains a stable center in the system (12).

The significant results here are the nonlinear terms and the potential for neutral stability (centers). For strategies prioritizing early resource gains, the evolutionary trajectory becomes highly sensitive to initial conditions, driving persistent oscillations in strategy frequencies. This provides a theoretical explanation for cyclical dynamics in natural systems, such as predator-prey cycles or cyclical competition among strategies. The RD (8) does not converge to a single static equilibrium, instead, past early competition exerts lasting effects on future evolution. This demonstrates the long-lasting inertial effect of historical resource advantages.

When $E_1(t) \geq K$ at time $t \geq t_1$, the instantaneous fitness is $\left(F_1^2(t)\right)' = \int_0^{t_1} f_1(\tau)d\tau + f_1(t)$. In the RD (8), the integral term represents the remaining historical resource retention, while the core driving term related to the frequency of strategies in evolutionary dynamics remains the current payoff difference, $f_1(t) - f_2(t)$. Its equilibria shift to $E_1^*(0,1)$, $E_2^*(1,0)$, $E_3^*\left(\frac{d-b-E_1(t_1)+E_2(t_1)}{a-b-c+d}, \frac{a-c+E_1(t_1)-E_2(t_1)}{a-b-c+d}\right)(\in [0,1], a-b-c+d \neq 0)$, whose stability characteristics align with those of classical RD (4). For capital breeders, saturation indicates that the period of capital accumulation has ended. The historical advantage, encapsulated in the integral term $\int_0^{t_1} f_1(\tau)d\tau$, becomes a frozen legacy. Selection pressure suddenly shifts from favoring phenotypes that excel at building capital to favoring those that are superior at exploiting resources immediately for real-time survival and reproduction. A strategy that was dominant during the accumulation phase may be replaced if it is not also the most effective in this new saturated environment.

Under the increasingly time-weighted RD (11), it is non-autonomous and explicitly depends on time t where $E_1(t) < K$. When $t = 0$, any $x(0) \in [0,1]$ satisfies $x' = 0$, so all $x(0)$ are equilibria. By contrast, when $t > 0$, the RD (11) has the equilibria E_1^*, E_2^*, E_3^* that do not change with time. As it is one-dimensional, all equilibria are nodes. The dynamic behavior of RD (11) is jointly governed by the sign and magnitude of $g_1(x)$ and time t. Because time t acts as a positive multiplication factor ($t > 0$), its positivity does not alter the sign of $g_1(x)$ but rather affects the magnitude of $\dot{x}$, i.e., the absolute value of $\dot{x}$ increases proportionally with time. Therefore, the stability analysis is similar to that of RD (4), both determined by $g_1'(x)$. Specifically, for $E_1^*(0,1)$, its eigenvalue is $\eta = t(b-d)$. When $b-d<0$, E_1^* is a stable node, otherwise it is an unstable node. For $E_2^*(1,0)$, its eigenvalue is $\eta = t(c-a)$. When $c-a<0$, E_1^* is a stable node, otherwise it is an unstable node. For $E_3^*\left(\frac{d-b}{a-b-c+d}, \frac{a-c}{a-b-c+d}\right)$, its eigenvalue is $\eta = t\frac{(d-b)(a-c)}{a-b-c+d}$. When $a < c \& d < b$, E_3^* is a stable node and when $a > c \& d > b$, it is a saddle. Besides, we analyze the effect of time on the convergence rate at the equilibria. By linearize the RD (11) around the stable equilibrium x^*, it gives $x'(t) = tg_1'(x^*)(x - x^*)$. Solving this linearized system yields $x(t) = x^* + (x(0) - x^*)\exp\left(\int_0^t g_1'(x^*)\iota d\iota\right) = x^* + (x(0) - x^*)\exp\left(\frac{g_1'(x^*)}{2}t^2\right)$. The convergence rate is dominated by the quadratic term in the exponential, i.e., $\left|\frac{g_1'(x^*)}{2}t^2\right|$.

The dynamics favor strategies that perform well at the end of the life stage. The stability analysis shows that selection pressures intensify over time, with time acting as a multiplicative factor. It models the physiology of pre-dormancy binge feeding in hibernators and of last-chance reproduction in semelparous species. In this context, natural selection is effectively myopic to the distant past, focusing intensely on the present. A strategy that performs poorly initially but superbly during the critical final phase may still be favored. This mode demonstrates how adaptation can be driven by brief, intense periods of selection rather than steady pressure throughout life.

When $E_1(t) \geq K$, the fitness simplifies to $\left(F_1^3(t)\right)' = f_1(t)$, at which the RD (11) reverts directly to the classical form. Thus, the equilibria and stability results are identical to the equilibria results of the equally time-weighted RD (4). For organisms that employ a final sprint strategy, reaching saturation often coincides with the onset of a critical life stage, such as entering hibernation or initiating reproduction. Active foraging ceases and survival then depends entirely on the output of accumulated reserves that have been mobilized. At this point, the evolutionary race is effectively over time t_1. The outcome is determined by the total capital $F_i^3(t) = \int_0^{t_1} \tau f_i(\tau)d\tau$ available for the ensuing challenge.

In summary, the stability analysis shows that time weighting fundamentally alters evolutionary dynamics. Equal weighting yields classical outcomes. Decreasing time-weighting introduces path dependence and neutral oscillations, which align with capital breeding strategies. By contrast, increasing time-weighting intensifies selection pressure over time, favoring strategies that excel in final resource acquisition. This is consistent with income breeding or critical life-stage sprint strategies. These theoretical predictions will be verified numerically in the next section.

3.2. Numerical simulations

In this section, we numerically simulate the cooperation behavior in several classical two-strategy games, including the Stag Hunt (SH), Snowdrift (SD), Prisoner's Dilemma (PD), and the Mixed Stable game (MS). The strategy set is $A = \{C, D\}$, where C and D

represent cooperation and defection, respectively. The payoff matrix is $M = \begin{pmatrix} 6 & \sigma \\ 6+\sigma & 2 \end{pmatrix}$. A tunable parameter σ governs the game type within the following ranges: a) SH when $\sigma \in (-\infty, 0]$, b) PD when $\sigma \in [0, 2]$, c) SD when $\sigma \in [2, 6]$, d) MS when $\sigma \in [6, \infty)$. The frequency $x(t)$ denotes the proportion of cooperators (C) and $1 - x(t)$ denotes the proportion of defectors (D) in the population at time t. The RDs for each time-weighted mode are simulated numerically using the ode solver in MATLAB. The average cooperation level $\langle \rho_c \rangle$ is calculated by averaging the strategy frequencies over the steady states, specifically from the last 400 time steps of a total simulation length of 20,400 steps. We denote the average cooperation levels for the equally, increasingly, and decreasingly time-weighted RDs as $\langle \rho_c^{eq.} \rangle$, $\langle \rho_c^{inc.} \rangle$, and $\langle \rho_c^{dec.} \rangle$, respectively.

When the resource reserve $E_1(t)$ remains below the maximum amount K ($E_1(t) < K$), the evolutionary outcomes of the different game types under the three time-weighted RDs are simulated, all starting from the same initial cooperation frequency $x(0) = 0.5$. Fig. 1 presents the results. Fig. 1(a) shows the average cooperation levels for the equally ($\langle \rho_c^{eq.} \rangle$), increasingly ($\langle \rho_c^{inc.} \rangle$), and decreasingly ($\langle \rho_c^{dec.} \rangle$) time-weighted RDs. Fig. 1(b) shows the differences in cooperation levels between these modes and the classical baseline $\Delta \langle \rho_c^{inc.} \rangle = \langle \rho_c^{inc.} \rangle - \langle \rho_c^{eq.} \rangle$ and $\Delta \langle \rho_c^{dec.} \rangle = \langle \rho_c^{dec.} \rangle - \langle \rho_c^{eq.} \rangle$. A striking result is that the average cooperation level under increasing time-weighting $\langle \rho_c^{inc.} \rangle$ (red dots) is consistently close to the classical baseline $\langle \rho_c^{eq.} \rangle$ (black dots), showing little difference. In stark contrast, the decreasingly time-weighted RD $\langle \rho_c^{dec.} \rangle$ produce markedly different outcomes. These results vary significantly with the initial change rate $x'(0) = 0$ (green dots) and $x'(0) = 0.5$ (purple dots) and the game parameter σ.

The dependence on initial conditions is a central finding. In the SH, $\langle \rho_c^{dec.} \rangle$ depends on both $x(0)$ and $x'(0)$, whereas $\langle \rho_c^{eq.} \rangle$ depends only on $x(0)$. A high initial change rate $x'(0) = 0.5$ allows cooperators to overcome the defectors' advantage and lead the population to full cooperation. In the PD, a high $x'(0)$ provides cooperators with a survival advantage when the temptation to defect c is low, enabling them to dominate and achieve $\langle \rho_c^{dec.} \rangle = 1$. However, defection remains dominant if c outweighs the reward for cooperation a. In the SD, $\langle \rho_c^{dec.} \rangle$ is improved compared to the classical baseline, with the degree of improvement varying with σ. As the dynamics approach the MS regime, the differences between the modes diminish.

A key finding is the elevated average cooperation level under decreasing time-weighting, particularly in the SD. This demonstrates that in environments where early investment is crucial, the historical legacy of cooperation can encourage ongoing cooperation, even in games with an inherent social dilemma. The RD avoids converging to a lower cooperation equilibrium, instead settling into a dynamic where the memory of past cooperative gains helps to sustain mutualism. In contrast, the minimal difference between equal and increasing time-weighting indicates that, in contexts prioritizing recent gains, the dynamics of cooperation do not differ substantially from the classical, memoryless RD.

To understand the sources of these differences, we examine the time series $x(t)$ for specific game parameters ($\sigma = -1, 1, 3, 5, 7$), focusing on the decreasingly time-weighted RDs as they exhibit the most significant deviations. Fig. 2 reveals the origin of the differences between $\langle \rho_c^{dec.} \rangle$ and $\langle \rho_c^{eq.} \rangle$. Surprisingly, the decreasingly time-weighted fitness induces oscillatory dynamics. In the SD and the MS, the cooperation frequency $x^{dec.}(t)$ oscillates regularly around the classical equilibrium $x^{eq.}(t)$. Furthermore, the period and amplitude of these oscillations depend on the game parameter σ and the initial conditions $x(0)$ and $x'(0)$.

This oscillatory optimization is particularly relevant in the SD, where a well-known social dilemma exists. While the collective

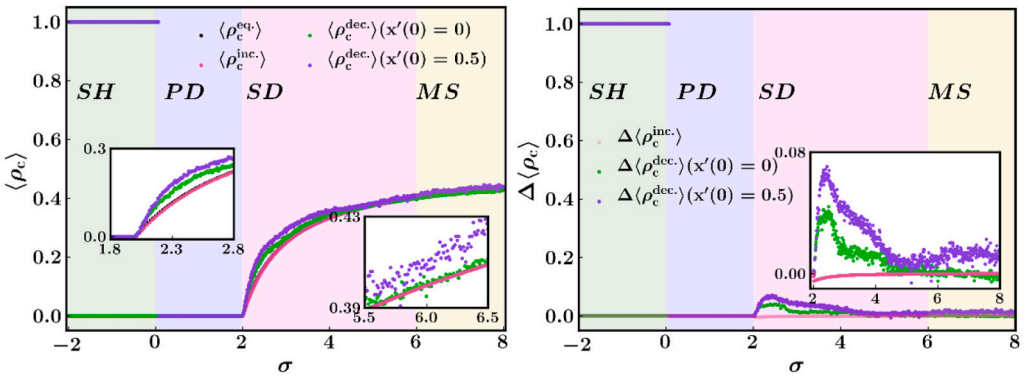

Fig. 1. (a) Average cooperation levels $\langle \rho_c \rangle$ and (b) their differences from the classical baseline$\Delta \langle \rho_c \rangle = \langle \rho_c \rangle - \langle \rho_c^{eq.} \rangle$ for three time-weighted replicator dynamics (RDs). Results are plotted as a function of the game parameter σ, with an initial cooperation frequency $x(0) = 0.5$ under unsaturated conditions $E_1(t) < K$. Game types: Stag Hunt (SH, $\sigma \in (-\infty, 0]$), Prisoner's Dilemma (PD, $\sigma \in (0, 2]$), Snowdrift (SD, $\sigma \in (2, 6]$), Mixed Stable (MS, $\sigma \in (6, \infty)$). Colors represent different time-weighting modes: black for equal weighting $\langle \rho_c^{eq.} \rangle$, red for increasing weighting $\langle \rho_c^{inc.} \rangle$, and green and purple for decreasing weighting $\langle \rho_c^{dec.} \rangle$ with $x'(0) = 0$ and $x'(0) = 0.5$. Decreasing time-weighting enhances cooperation, while increasing time-weighting yields outcomes similar to the classical model. (For interpretation of the references to colour in this figure legend, the reader is referred to the web version of this article.)

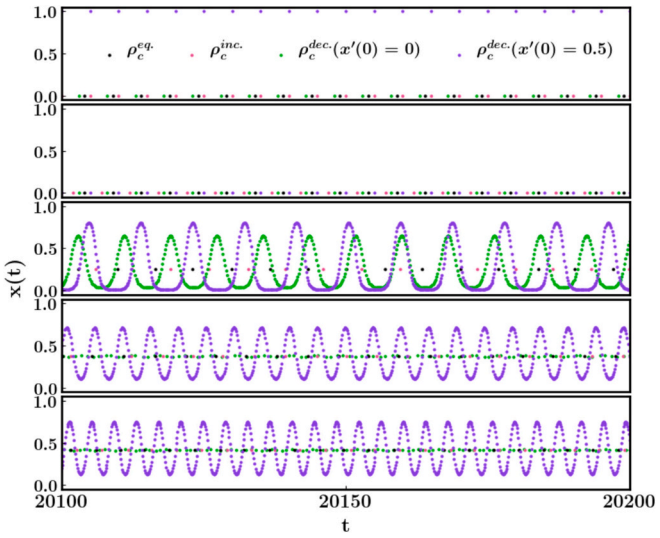

Fig. 2. Time series of cooperation frequencies $x(t)$ for three time-weighted RDs with $x(0) = 0.5$ and $E_1(t) < K$. Rows show different game types (from top to bottom): SH ($\sigma = -1$), PD ($\sigma = 1$), SD ($\sigma = 3,5$), and MS ($\sigma = 7$). Colors represent different time-weighting modes: black for equal weighting, red for increasing weighting, and green and purple for decreasing weighting with $x'(0) = 0$ and $x'(0) = 0.5$. Decreasing time-weighting induces persistent oscillations in the SD and the MS, whereas other modes converge to stable equilibria. (For interpretation of the references to colour in this figure legend, the reader is referred to the web version of this article.)

payoff increases with the cooperation level, cooperators receive a lower payoff than defectors when the cooperation level falls below a critical threshold $\langle \rho_c^{eq.} \rangle$. This incentivizes individuals to prioritize short-term self-interest. Our simulations demonstrate that the average cooperation level can be enhanced through these oscillations. For a fixed σ, the trajectory oscillates above and below $x^{eq.}(t)$, suggesting that there are optimal time windows where the reinforcement of cooperation is maximized.

The sustained oscillations in cooperation are not just a mathematical curiosity. They could be a mechanism that explains the cyclical dynamics commonly observed in nature, such as predator-prey cycles and parasite-host coevolution. The mechanism underlying these cycles is rooted in historical resource metabolism. The high value placed on early gains creates an inertial effect. A strategy that gains an initial advantage maintains a high cumulative fitness $F_1^2(t)$, which buffers it against short-term setbacks. If this advantage is not absolute, the disadvantaged strategy can gradually recover, leading to phases of alternating dominance. This provides a novel game-theoretic explanation of population cycles is driven by the internal dynamics of resource metabolism and historical competition, rather than by external environmental factors.

The initial conditions exert distinct effects across different game types when $E_1(t) < K$. Fig. 3 illustrates how the average cooperation levels vary with the game parameter σ under different initial cooperation frequency $x(0) \in [0,1]$. Fig. 3(a) presents the results for the equally and increasingly time-weighted RDs, which show no dependence on the initial frequency $x(0)$. Fig. 3(b) and (c) reveal the strong influence of $x(0)$ on the decreasingly time-weighted RD under different initial change rates $x'(0) = 0$ and $x'(0) = 0.5$. An outstanding result is observed in Fig. 3 (c). Under decreasing time-weighting with a positive initial change rate $x'(0) = 0.5$, cooperators achieve full dominance $\langle \rho_c^{dec.} \rangle = 1$ for any initial frequency $x(0)$ in the SH and for a range of $x(0)$ in the PD with low temptation. This demonstrates the ability of historical advantages to overcome social dilemmas. In the SD and the MS, the average cooperation level $\langle \rho_c^{dec.} \rangle$ is enhanced across most initial conditions, with higher values typically observed for extreme $x(0)$ values and under $x'(0) = 0.5$.

To elucidate the mechanisms behind these increases, Fig. 4 analyzes the period and amplitude of oscillations in the decreasingly time-weighted RD. In the SH and the PD, the dynamics converge to stable equilibria. In contrast, the SD and the MS exhibit nonlinear oscillations whose properties vary with σ and $x(0)$. Under $x'(0) = 0$ (Fig. 4 (a)(b)): Period decreases monotonically with σ. Amplitude displays a more complex relationship: it increases at small $x(0)$, decreases at large $x(0)$, and exhibits non-monotonic behavior at intermediate $x(0)$. Both period and amplitude are down-convex functions of $x(0)$ for a fixed σ, but their minima occur at different locations. Under $x'(0) = 0.5$ (Fig. 4 (c)(d)), the period decreases and the amplitude increases universally compared to the $x'(0) = 0$ case. Furthermore, the patterns of period and amplitude become symmetric about $x(0) = 0.5$. This symmetry and increased oscillation magnitude explain the enhanced average cooperation levels shown in Fig. 1.

Fig. 5 provides a comprehensive view by mapping $\langle \rho_c^{dec.} \rangle$, period, and amplitude as functions of both the initial change rate $x'(0) \in [-1,1]$ and the game parameter σ, for a fixed $x(0) = 0.5$. The analysis confirms that a positive initial change rate $x'(0) > 0$ above a critical threshold can solve cooperation dilemmas in the SH and the PD, enabling a transition from full defection (dark blue) to full cooperation (dark red) in Fig. 5 (a). In the SD and the MS, all three metrics $\langle \rho_c^{dec.} \rangle$, period, and amplitude are symmetric about $x'(0) = 0$. Their values increase with $|x'(0)|$, consistent with the squared $x'(0)$ term in the dynamics. Both period and amplitude decrease with increasing σ. Near $x'(0) = 0$ and for large σ, the nonlinear term diminishes, explaining the transition from oscillations to near-

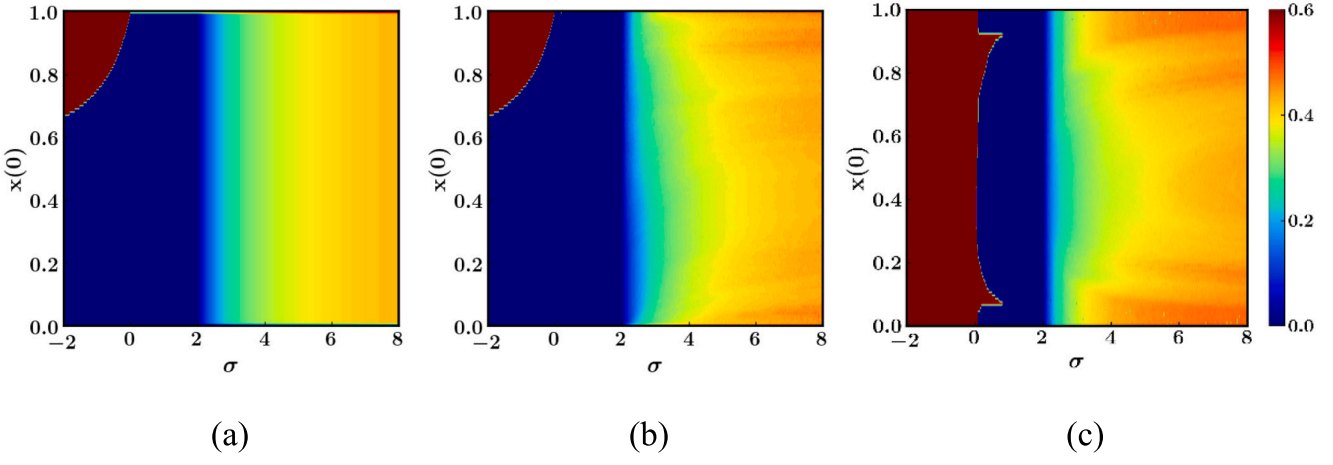

Fig. 3. Average cooperation levels $\langle \rho_c \rangle$ for three time-weighted replicator dynamics (RDs) with $E_1(t) < K$. Heatmaps are plotted as a function of the game parameter σ and initial cooperation frequency $x(0) \in [0, 1]$, (a) equally and increasingly time-weighted RDs, (b) decreasingly time-weighted RD with $x^{'}(0) = 0$, and (c) decreasingly time-weighted RD with $x^{'}(0) = 0.5$. The colour scale ranges from dark red, denoting full cooperation $\langle \rho_c \rangle = 1$, to dark blue, denoting full defection $\langle \rho_c \rangle = 0$. Decreasingly time-weighted RD with $x^{'}(0) = 0.5$ enables full cooperation across all $x(0)$ in the SH and for a range of $x(0)$ in the PD, whereas equally and increasingly time-weighted RDs show no dependence on initial $x(0)$. (For interpretation of the references to colour in this figure legend, the reader is referred to the web version of this article.)

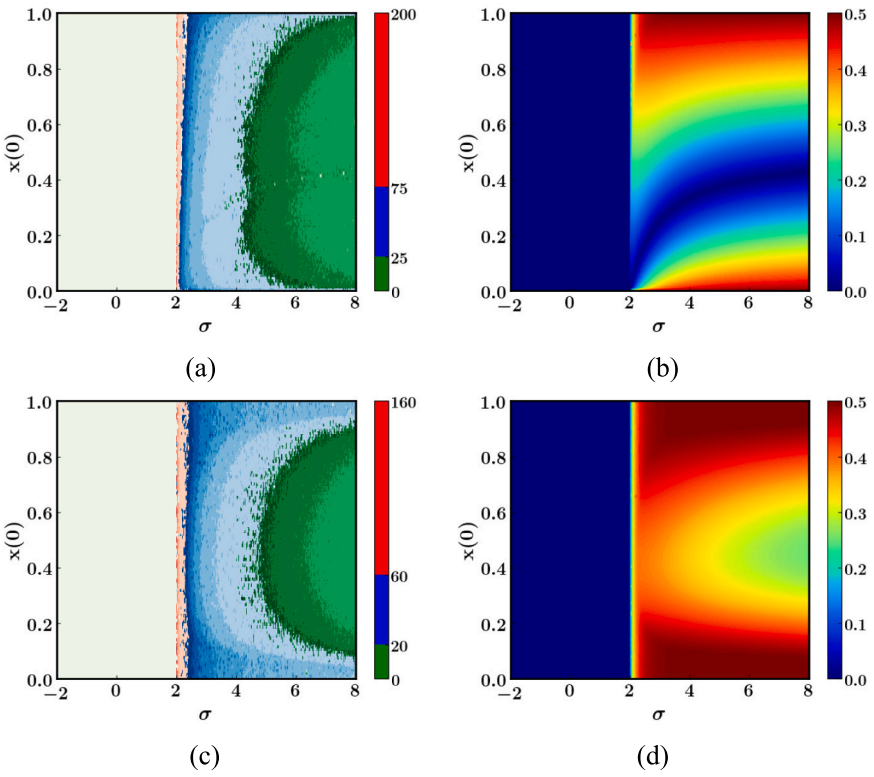

Fig. 4. Period (a, c) and amplitude (b, d) of steady-state oscillations in decreasingly time-weighted RDs under $E_1(t) < K$ as functions of the initial cooperation frequency $x(0) \in [0, 1]$ and the game parameter σ. Upper panels: an initial change rate $x^{'}(0) = 0$; Lower panels: $x^{'}(0) = 0.5$. Darker colors indicate larger values of period or amplitude. Oscillations occur primarily in the SD and the MS, where both period and amplitude vary nonlinearly with σ. $x^{'}(0) = 0.5$ induces symmetric patterns around $x(0) = 0.5$, enhancing cooperation via larger amplitude at extreme initial frequencies.

equilibrium dynamics observed in Fig. 2.

The strong dependence on initial conditions, particularly the initial change rate $x^{'}(t)$ is a profound insight under decreasing time-weighting. This implies that the evolutionary trajectories of a population are path-dependent. A population's history, not just its current state, casts a long shadow over its future. An early head advantage in acquiring resources (a positive initial change rate for cooperators $x^{'}(0)$) can permanently alter the evolutionary outcome, even escaping defective traps in the PD. This mirrors the ecological concept of positive feedback and highlights the critical role of historical contingency in evolution, where initial successes beget further success through the inertial effect of accumulated resources.

Finally, Fig. 6 compares the convergence rates of the time-weighted RDs across different game types when $E_1(t) < K$. The figure displays initial transients for the SH ($\sigma = -1$), the PD ($\sigma = 1$), the SD ($\sigma = 3$ and $\sigma = 5$), and the MS ($\sigma = 7$). In all cases, the increasingly time-weighted RD (red line) converges faster than the other dynamics (black, green, and purple lines), confirming the theoretical predictions of Sec. 3.1. This accelerated convergence occurs because this mode prioritizes recent gains, allowing the most efficient current strategy to dominate unencumbered by historical inertia. A second key result emerges in the PD that the decreasingly time-weighted RDs exhibit a strong transient surge in cooperation before eventually declining to full defection. This indicates that an initial period of high cooperation can provide a robust, albeit temporary, defense against defectors. This transient cooperative state represents a form of ecological buffering. It provides a biological opportunity whereby a population may sustain a high level of cooperation long enough to overcome a critical challenge. In a finite time horizon or a periodically changing environment, this temporary state could be sufficient for colonizing a new habitat, surviving a harsh season, or achieving a quorum for collective defense.

Unlike the results under unsaturated conditions $E_1(t) < K$ (Figs. 1–6), our theoretical analysis (Sec. 2 and Sec. 3.1) indicates that time-weighted RDs revert to the classical form when the resource reserve reaches the maximum amount $E_1(t) \geq K$. Therefore, we investigate the evolutionary transition from unsaturated to saturated states. A key factor governing this process is the maximum amount, defined as $K = \lambda \cdot T \cdot R_{max}$, where $R_{max} = max\{a, b, c, d\}$ is the maximum payoff per game, T is the life stage duration, and λ is the storage efficiency coefficient. Since the equally time-weighted RD is unaffected by K, we focuses on the increasingly and decreasingly time-weighted modes.

Fig. 7 illustrates the transient dynamics of cooperation frequencies within the first 15 time steps, highlighting the effects of life stage duration T and storage efficiency λ across game types, with $x(0) = 0.5$. Fig. 7 (a) and (b) correspond to decreasingly time-weighted RD with $x^{'}(0) = 0.5$. In Fig. 7(a), under a fixed $\lambda = 0.5$, the black curve represents the unsaturated baseline $E_1(t) < K$,

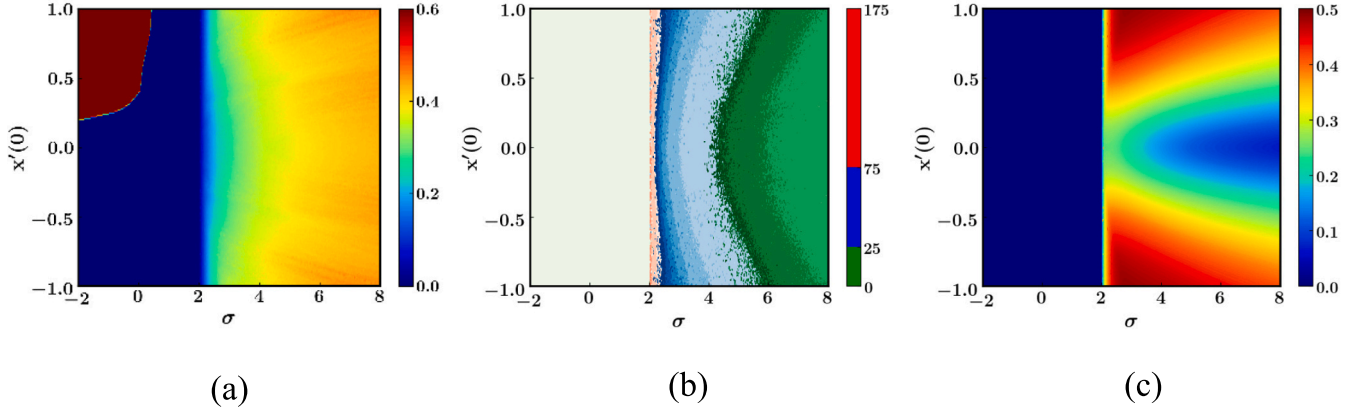

Fig. 5. (a) Average cooperation levels, (b) period, and (c) amplitude in decreasingly time-weighted RDs with $x(0) = 0.5$ and $E_1(t) < K$ as functions of initial cooperation rate $x'(0) \in [-1, 1]$ and the game parameter σ (from SH to MS as defined in Fig. 1). (a) Colour from dark red (full cooperation) to dark blue (full defection); (b, c) darker colors indicate larger periods or amplitudes. A positive $x'(0)$ above a threshold solves cooperation dilemmas in the SH and the PD. In the SD and the MS, oscillations are symmetric around $x'(0) = 0$, and larger $|x'(0)|$ enhance cooperation. (For interpretation of the references to colour in this figure legend, the reader is referred to the web version of this article.)

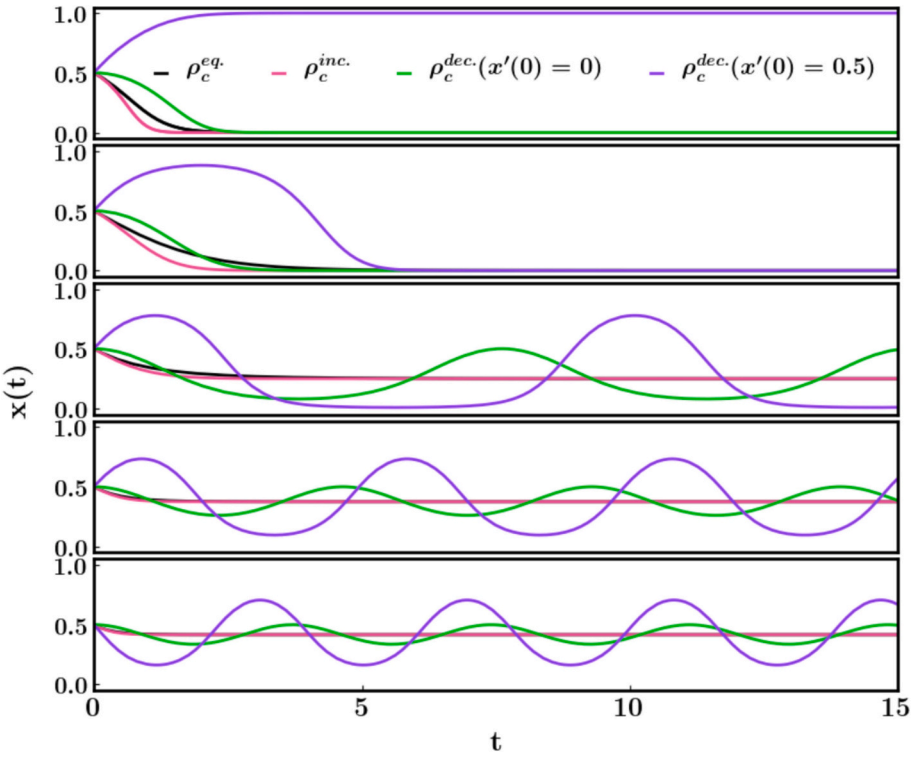

Fig. 6. Transient cooperation frequencies $x(t)$ within the first 15 time steps for three time-weighted RDs with $x(0) = 0.5$ and $E_1(t) < K$. Rows show different game types (from top to bottom): SH ($\sigma = -1$), PD ($\sigma = 1$), SD ($\sigma = 3, 5$), and MS ($\sigma = 7$). Colors represent different time-weighting modes: black for equal weighting, red for increasing weighting, and green and purple for decreasing weighting with $x'(0) = 0$ and $x'(0) = 0.5$. Increasingly time-weighted RDs converge fastest. Decreasingly weighted RDs show a transient cooperation boost in the PD and sustained oscillations in the SD and MS. (For interpretation of the references to colour in this figure legend, the reader is referred to the web version of this article.)

while the colored curves show dynamics after saturation $E_1(t) \geq K$ at different T. Notably, shorter life stages ($T = 1$) accelerate the decline in cooperation frequency. In the SD and the MS, this eliminates the oscillatory coexistence observed in the unsaturated state, as populations rapidly shift toward defection. In Fig. 7(b), with a fixed $T = 2$, lower storage efficiency $\lambda = 0.1$ accelerates the shift to defection upon saturation compared to higher efficiency $\lambda = 0.9$. This reflects the physiological constraints that organisms with low λ cannot maintain sufficient reserves and must rely more on immediate gains, undermining cooperation.

Fig. 7(c) and (d) show the results of the increasingly time-weighted RD. In contrast, the cooperation dynamics show minimal sensitivity to T and λ. Regardless of parameter variations, the evolution trajectories under saturation closely track those under unsaturated conditions, converging to the same equilibrium. This robustness arises because this mode prioritizes recent resource gains, the contribution of which depends weakly on total reserve capacity or stage duration. This aligns with the behavior of hibernators that prioritize pre-dormancy hyperphagia over long-term storage.

The dramatic dynamical shift upon saturation highlights a fundamental trade-off in life history. For decreasing time-weighting, saturation forces a strategic transition from a capital accumulator to a scramble competitor. This abrupt change eliminates oscillatory coexistence, favoring defectors that excel in short-term competition. This models scenarios where a finite growth season ends, forcing a switch from building reserves to surviving on immediate finds. For increasing time-weighting, the strategy is robust to saturation. This confirms that for final sprint strategists, maximizing intake during the critical window is key. Their overall storage capacity is less important than the efficiency of that final effort.

Thus, the maximum amount K is not merely a physiological constraint but a switch between distinct regimes of natural selection. A small K (from short T or low λ) forces a population rapidly into an income-breeding regime, favoring defectors. Conversely, a large K (from long T or high λ) permits an extended period of capital accumulation, favoring cooperators that benefit from the long-term, time-weighted returns on cooperation.

4. Conclusions and discussions

In this study, we have developed a novel time-weighted fitness framework that integrates resource storage, metabolism and historical payoffs into evolutionary game theory. By decomposing fitness into three levels including resource acquisition, cumulative fitness, and instantaneous fitness, we derived extended replicator dynamics that capture how organisms manage energy at different life stages in ecological reality. Our analysis reveals that how resources are weighted over time (equal, decreasing or increasing amounts) is

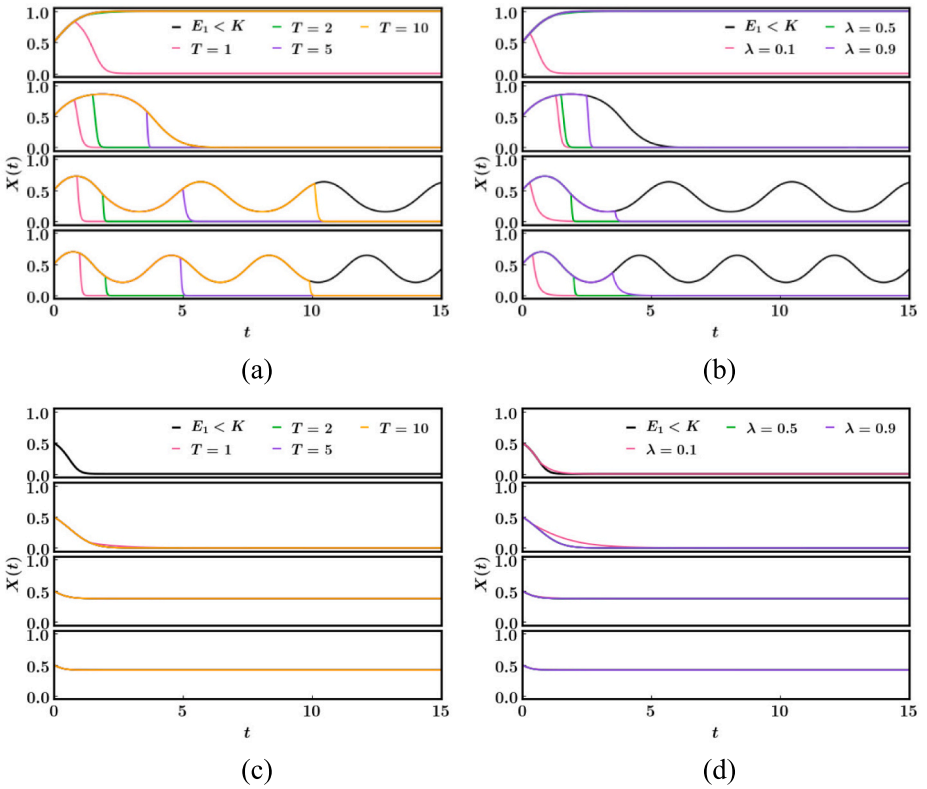

Fig. 7. Transient cooperation frequencies $x(t)$ within the first 15 time steps for two time-weighted RDs with the initial cooperation frequency $x(0) = 0.5$ under saturated conditions $E_1(t) \geq K$. Rows in every panel show different game types (from top to bottom): SH ($\sigma = -1$), PD ($\sigma = 1$), SD ($\sigma = 5$), and MS ($\sigma = 7$). Symbols: black lines for unsaturated baseline $E_1(t) < K$; colored lines for $E_1(t) \geq K$. Decreasingly time-weighted RDs ($x'(0) = 0.5$): (a) Varying life stage duration T ($\lambda = 0.5$); (b) Varying storage efficiency λ ($T = 2$). (c, d) Increasingly time-weighted RDs. Saturation accelerates the shift to defection for decreasing time-weighting, eliminating oscillations; increasing time-weighting is robust to parameter changes.

a key factor in determining evolutionary outcomes. This weighting mechanism gives rise to dynamics absent in classical models, most notably persistent oscillations and strong path dependence. These phenomena were previously observed primarily in discrete-time models [31] or in spatially structured populations [32]. Our framework demonstrates that they can emerge from temporal resource metabolism in well-mixed populations.

The most significant implication of our work is that it unifies historical contingency with instantaneous selection. We have demonstrated that while natural selection acts on the present, the present is profoundly influenced by the past. This resolves the apparent paradox between the immediate action of selection and the long-term legacy of resource accumulation. Our framework provides a mechanistic, game-theoretic basis for diverse ecological phenomena, from the capital breeding strategy of Svalbard reindeer (explained by decreasing time-weighting), to the binge-feeding physiology of hibernators (explained by increasing time-weighting) [21,23,30]. The closed feedback loop between payoffs, resources, metabolism and strategy formalizes the concept of an individual's changing physiological state as a core driver of frequency-dependent selection.

However, our model inevitably has limitations that present opportunities for future research. First, while the assumption of linear weighting functions provides analytical tractability, it oversimplifies nonlinear metabolic processes such as sharp torpor transitions [33]. Future work could implement nonlinear functions to model specific biological systems more accurately. Second, our model examines a single life stage with a consistent metabolic strategy. Throughout their lifetime, however, organisms undergo multiple stages (e.g. juvenile growth and adult reproduction) with distinct metabolic priorities. Future research could embed our stage-specific framework into a larger meta-model, in which the time-weighted mode evolves or switches in response to major life-history transitions. Finally, our framework currently assumes a well-mixed population in a static environment. Promising extensions include integrating spatial structure and social networks to study the interaction between local resource competition, dispersal, and temporal weighting [34,35]. A separate, valuable avenue would be to incorporate explicit environmental fluctuation, exploring how the optimal time-weighting mode itself might evolve in response to predictable or stochastic cycles.

In summary, this study bridges the gap between evolutionary game theory and life-history ecology by formalizing how the metabolism of historical resources drives the evolution of strategies. The framework shifts the focus from identifying an optimal strategy to understanding how the timing of resource acquisition and the physiological capacity for storage shape the paths that evolution can take. This perspective opens up new avenues for understanding adaptive strategies across diverse temporal scales and

ecological contexts.

CRediT authorship contribution statement

Yanyan Han: Writing – review & editing, Writing – original draft, Visualization, Validation, Methodology, Formal analysis, Conceptualization. **Minlan Li:** Writing – review & editing, Validation, Methodology, Funding acquisition, Conceptualization. **Xuemeng Song:** Writing – original draft, Visualization, Conceptualization. **Jia-Xu Han:** Writing – review & editing, Methodology. **Feng Zhang:** Writing – review & editing, Validation, Methodology, Conceptualization. **Rui-Wu Wang:** Writing – review & editing, Validation, Supervision, Resources, Funding acquisition, Conceptualization.

Declaration of competing interest

The authors declare that they have no known competing financial interests or personal relationships that could have appeared to influence the work reported in this paper.

Acknowledgements

This work was supported by the National Natural Science Foundation of China–Yunnan Joint Fund (U2102221) and the Shaanxi Provincial Postdoctoral Scientific Research Project Funding (2024BSHSDZZ004).

Appendix A. Supplementary data

The code used to implement the extended replicator dynamics and generate the results is available. https://github.com/YYHan224/Time-Weighted-Evolutionary-Games.git. Supplementary data to this article can be found online at doi:https://doi.org/10.1016/j.chaos.2025.117236.

Data availability

No data was used for the research described in the article.

References

[1] Darwin CR. On the origin of species by means of natural selection, or the preservation of favoured races in the struggle for life. John Murray; 1859.
[2] Page KM, Nowak MA. Unifying evolutionary dynamics. J Theoret Biol 2002;219(1):93–8. https://doi.org/10.1006/jtbi.2002.3112.
[3] Taylor PD, Jonker LB. Evolutionary stable strategies and game dynamics. Math Biosci 1978;40(1):45–56. https://doi.org/10.1016/0025-5564(78)90077-9.
[4] Li ML, Liu YP, Han YY, Wang RW. Environmental heterogeneity unifies the effect of spatial structure on the altruistic cooperation in game-theory paradigms. Chaos, Solitons Fractals 2022;163:112595. https://doi.org/10.1016/j.chaos.2022.112595.
[5] Wadgymar SM, Sheth S, Josephs E, DeMarche M, Anderson J. Defining fitness in evolutionary ecology. Int J Plant Sci 2024;185(3):218–27. https://doi.org/10.1086/729360.
[6] Stephens PA, Boyd IL, McNamara JM, Houston AI. Capital breeding and income breeding: their meaning, measurement, and worth. Ecology 2009;90(8):2057–67. https://doi.org/10.1890/08-1369.1.
[7] Glynatsi NE, Akin E, Nowak MA, Hilbe C. Conditional cooperation with longer memory. Proc Natl Acad Sci USA 2024;121(50):e2420125121. https://doi.org/10.1073/pnas.2420125121.
[8] Han JX, Bai ZD, Wang RW. Evolutionary history mediates adaptation through shaping genetic variance. J Syst Evol 2025;63(4):910–21. https://doi.org/10.1111/jse.13163.
[9] Tao Y, Wang Z. Effect of time delay and evolutionarily stable strategy. J Theoret Biol 1997;187(1):111–6. https://doi.org/10.1006/jtbi.1997.0427.
[10] Yuan H, Meng X. Replicator dynamics of division of labor games with delayed payoffs in infinite populations. Chaos, Solitons Fractals 2022;158:112058. https://doi.org/10.1016/j.chaos.2022.112058.
[11] Wettergren TA. Replicator dynamics of evolutionary games with different delays on costs and benefits. Appl Math Comput 2023;458:128228. https://doi.org/10.1016/j.amc.2023.128228.
[12] Wang XW, Nie S, Jiang LL, Wang BH, Chen SM. Cooperation in spatial evolutionary games with historical payoffs. Phys Lett A 2016;380(36):2819–22. https://doi.org/10.1016/j.physleta.2016.06.026.
[13] Duan Y, Huang J, Zhang J. Evolutionary public good games based on the long-term payoff mechanism in heterogeneous networks. Chaos, Solitons Fractals 2023;174:113862. https://doi.org/10.1016/j.chaos.2023.113862.
[14] Li D, Zhou K, Sun M, Han D. Investigating the effectiveness of individuals' historical memory for the evolution of the prisoner's dilemma game. Chaos, Solitons Fractals 2023;170:113408. https://doi.org/10.1016/j.chaos.2023.113408.
[15] Zhang Y, Wang J, Wen G, Guan J, Zhou S, Chen G. Limitation of time promotes cooperation in structured collaboration systems. IEEE Trans Netw Sci Eng 2025;12(1):4–12. https://doi.org/10.1109/TNSE.2024.3481434.
[16] Du WB, Cao XB, Liu RR, Jia CX. The effect of a history-fitness-based updating rule on evolutionary games. Int J Mode Phys C 2010;21(12):1433–42. https://doi.org/10.1142/S0129183110015956.
[17] Utsumi S, Tatsukawa Y, Tanimoto J. Does a resource-storing mechanism favor "the wealthy do not fight"?—an approach from evolutionary game theory. Chaos, Solitons Fractals 2022;160:112207. https://doi.org/10.1016/j.chaos.2022.112207.
[18] Kabir KMA, Islam MDS, Utsumi S, Tanimoto J. The emergence of rich complex dynamics in a spatial dyadic game with resource storage, participation cost, and agent interaction propensity. Chaos, Solitons Fractals 2023;175:114035. https://doi.org/10.1016/j.chaos.2023.114035.
[19] Liu Y, Li Y. A payoff equality perspective for evolutionary games: mental accounting and cooperation promotion. Appl Math Comput 2025;486:129039. https://doi.org/10.1016/j.amc.2024.129039.

[20] Kooijman B. Dynamic energy budget theory for metabolic organisation. 3rd ed. Cambridge University Press; 2009. https://doi.org/10.1017/CBO9780511805400.
[21] Veiberg V, Loe LE, Albon SD, Irvine RJ, Tveraa T, Ropstad E, et al. Maternal winter body mass and not spring phenology determine annual calf production in an Arctic herbivore. Oikos 2017;126(7):980–7. https://doi.org/10.1111/oik.03815.
[22] Sibly RM, Hone J, Clutton–Brock TH, Clutton–Brock TH, Coulson T. Comparative ungulate dynamics: the devil is in the detail. Philos Trans R Soc Lond B 2002;357(1425):1285–98. doi: https://doi.org/10.1098/rstb.2002.1128.
[23] Wang LCH, Lee T. Torpor and hibernation in mammals: metabolic, physiological, and biochemical adaptations. Comp Physiol 2011:507–32. https://doi.org/10.1002/cphy.cp040122.
[24] Giroud S, Habold C, Nespolo RF, Mejías C, Terrien J, Logan SM, et al. The torpid state: recent advances in metabolic adaptations and protective mechanisms. Front Physiol 2021;11:623665. https://doi.org/10.3389/fphys.2020.623665.
[25] Brown JH, Gillooly JF, Allen AP, Savage VM, West GB. Toward a metabolic theory of ecology. Ecology 2004;85(7):1771–89. https://doi.org/10.1890/03-9000.
[26] Laraki R, Mertikopoulos P. Higher order game dynamics. J Econ Theory 2013;148(6):2666–95. https://doi.org/10.1016/j.jet.2013.08.002.
[27] Hofbauer J, Sorin S, Viossat Y. Time average replicator and best-reply dynamics. Math Oper Res 2009;34(2):263–9. https://doi.org/10.1287/moor.1080.0359.
[28] Nowak MA. Evolutionary dynamics. Cambridge: Harvard University Press; 2006.
[29] Guckenheimer J, Holmes P. Nonlinear oscillations, dynamical systems, and bifurcations of vector fields. New York: Springer; 2013. https://doi.org/10.1007/978-1-4612-1140-2.
[30] Gamelon M, Focardi S, Baubet E, Brandt S, Franzetti B, Ronchi F, et al. Reproductive allocation in pulsed-resource environments: a comparative study in two populations of wild boar. Oecologia 2017;183:1065–76. https://doi.org/10.1007/s00442-017-3821-8.
[31] Varun P, Archan M, Sagar C. Weight of fitness deviation governs strict physical chaos in replicator dynamics. Chaos 2018;28(3):033104. https://doi.org/10.1063/1.5011955.
[32] Zhang SP, Zhang JQ, Chen L, Liu XD. Oscillatory evolution of collective behavior in evolutionary games played with reinforcement learning. Nonlinear Dyn 2020;99:3301–12. https://doi.org/10.1007/s11071-019-05398-4.
[33] Zhang X, Tilling K, Martin RM, Oken E, Naimi AI, Aris IM, et al. Analysis of 'sensitive' periods of fetal and child growth Free. Int J Epidemiol 2019;48(1):116–23. https://doi.org/10.1093/ije/dyy045.
[34] Huang J, Zhu Y, Zhao D, Xia C, Perc M. The impact of feedbacks on evolutionary game dynamics in structured populations. Chaos 2025;35(6):063134. https://doi.org/10.1063/5.0278673.
[35] Zhang G, Xiong X, Pi B, Feng M, Perc M. Spatial public goods games with queueing and reputation. Appl Math Comput 2025;505:129533. https://doi.org/10.1016/j.amc.2025.129533.